Dynamic Light Scattering Investigations of Human Erythrocyte Spectrin†

Donna M. Budzynski,‡ Albert S. Benight,‡ Cynthia C. LaBrake,§ and L. W.-M. Fung*,§

Department of Chemistry, MC 111, Box 4348, University of Illinois at Chicago, Chicago, Illinois 60680, and Department of Chemistry, Loyola University of Chicago, Chicago, Illinois 60626

Received July 25, 1991; Revised Manuscript Received January 30, 1992

ABSTRACT: Dynamic light scattering measurements were performed on spectrin from human erythrocytes in 25 mM Tris buffer at pH 7.6 with 100 mM NaCl and 5 mM EDTA. Measurements were made on spectrin solutions prepared as dimers and tetramers over the temperature range from 23 to 41 °C, as a function of the square of the scattering vector ($\mathbf{K}^2$) over the range of 0.7×10^{10} cm$^{-2} \leq \mathbf{K}^2 \leq 20 \times 10^{10}$ cm^{-2}. Analysis of the autocorrelation functions collected for these solutions revealed the presence of two predominant motional components over the entire range of $\mathbf{K}^2$. Plots of the diffusion coefficients (D_{20}) of these components, with viscosity and temperature corrected to water at 20 °C, as a function of $\mathbf{K}^2$ indicated three rather distinct regions, flat regions at low and high $\mathbf{K}^2$ joined by a sloping intermediate region. At small $\mathbf{K}^2$ ($\leq 4 \times 10^{10}$ cm^{-2}) the D_{20} values were $(7.3 \pm 2.0) \times 10^{-8}$ cm^2/s for the slow component and $(20.3 \pm 2.0) \times 10^{-8}$ cm^2/s for the fast component. At large $\mathbf{K}^2$ ($\geq 10 \times 10^{10}$ cm^{-2}) the values increased to $(13.0 \pm 2.0) \times 10^{-8}$ cm^2/s for the slow component and $(39.4 \pm 2.0) \times 10^{-8}$ cm^2/s for the fast component. In the intermediate $\mathbf{K}^2$ region, D_{20} is a linear function of $\mathbf{K}^2$ and appears as a transition between the low and high $\mathbf{K}^2$ regions. The behaviors of the fast and slow components as a function of $\mathbf{K}^2$ were interpreted in terms of spectrin motions by modeling spectrin heterodimers and tetramers as wormlike coils. In the low $\mathbf{K}^2$ region the slow [$(7.3 \pm 2.0) \times 10^8$ cm^2/s] and fast [$(20.3 \pm 2.0) \times 10^{-8}$ cm^2/s] components were assigned to the center of mass diffusion coefficients (D_0) for tetramers (D_0^{tet}) and dimers (D_0^{dim}), respectively. In the high $\mathbf{K}^2$ region, the slow component was attributed to an average of D_0^{tet} and D_0^{dim}. The magnitude of D_{20} of the fast component [$(39.4 \pm 2.0) \times 10^{-8}$ cm^2/s] suggested the emergence of much faster motions, surmised to be subglobal segmental motions of spectrin tetramers. These measurements supply further evidence for fluctuational segmental motions of spectrin that occur over a relatively large distance of 22–30 nm with relaxation times ≤ 23 μs.

Spectrin is a major protein in the human erythrocyte membrane skeleton (Bennett & Lambert, 1991). It plays an integral role in determining the mechanical properties and maintaining the unique bioconcave shape of the erythrocyte. Spectrin consists of a heterodimer comprised of α with a molecular weight of about 285 000 (Sahr et al., 1990) and β with a molecular weight of about 246 000 (Winkelmann et al., 1990) subunits, associated side to side in an antiparallel helical orientation (Shotton et al., 1979). The dimers associate in a head-to-head manner resulting in tetramers. In solution, the dimer to tetramer equilibrium is highly temperature dependent (Ungewickell & Gratzer, 1978; Stokke et al., 1985; Shahbakthti & Gratzer, 1988; Morris & Ralston, 1989; Ralston, 1991). The dimers in solution are highly flexible with a maximum extended contour length of approximately 100 nm, and the tetramers have a maximum extended contour length of about 200 nm, as visualized by electron microscopy (EM) (Shotton et al., 1979; Byers & Branton, 1985; Elgsaeter et al., 1986). Circular dichroism measurements of spectrin dimers indicated 65–70% α-helical content (Ralston, 1978; Calvert et al., 1980). In solution in the absence of any other protein components, spectrin dimers and tetramers have been proposed to adopt a wormlike coil configuration with root mean square (rms) end-to-end distances of about 53 nm for the dimer and 82 nm for the tetramer (Stokke et al., 1985; Elgsaeter et al., 1986). Calculations show that the average end-to-end distance of the tetramer in the native skeleton of human erythrocytes is about 70 nm (Vertessy & Steck, 1989). On the basis of data obtained from yield shear resultant and plastic viscosity studies, a "spring" model has been proposed (Waugh, 1982). In this model, the unstressed state of the spectrin tetramer exists in a coiled conformation, such that the end-to-end distance is about 76 nm. Reversible conformational changes occur when the end-to-end distance changes but does not exceed 200 nm. It is suggested that mechanical forces rupture intramolecular bonds within the spectrin molecules when the molecule approaches its fully extended length. Recent electron micrographs of partially extended tetramers show that the two subunits are twisted about a common axis, and by varying the pitch and diameter of the two-stranded helical particle, their dimensions can be extended or condensed. According to this model, the native spectrin tetramer would have 10 turns with a pitch of 7 nm and a diameter of 5.9 nm (McGough & Josephs, 1990).

Amino acid sequence (Speicher et al., 1983) and cDNA sequence (Sahr et al., 1990; Winkelmann et al., 1990) analyses revealed that about 90% of spectrin, by mass, is comprised of repetitive structural units of 106 amino acid residues. Other spectrin-like proteins, including brain spectrin (Wasenius et al., 1989), dystrophin (Davison & Critchley, 1989; Koenig, 1988), and α-actinin (Davison et al., 1989) also have similar repetitive units. On the basis of the assumption that the 106 residues form the basic structural domain for spectrin, a simple and attractive triple-helical structure (Speicher & Marchesi, 1984), or a more detailed 5-fold structure (Xu et al., 1990), has been proposed.

Hydrodynamic, light scattering, birefringence relaxation, and viscometric studies support the view that spectrin molecules are long and flexible (Ralston, 1976; Elgsaeter, 1978; Mikkelsen & Elgsaeter, 1978, 1981). Hydrodynamic studies

† This work was supported by NIH Grants R29-GM49371 (A.S.B.) and R01-38361 and S15-HL41756 (L.W.-M.F.) and NSF Grant DMB-9018782 (A.S.B.).

* Address correspondence to this author.

‡ University of Illinois at Chicago.

§ Loyola University of Chicago.

0006-2960/92/0431-3653$03.00/0

of spectrin tetramers by analytical ultracentrifugation gave a diffusion coefficient of 11×10^{-8} cm^2/s (Ralston, 1976). Using total intensity light scattering techniques, Elgsaeter (1978) found the radius of gyration, R_G, of the dimer in 100 mM NaCl solution to be about 22 nm. R_G was found to nearly double at low ionic strength (1 mM NaCl solution), indicating an even more extended molecule in these conditions. Electric birefringence relaxation studies (Mikkelsen & Elgsaeter, 1978), measurements of the rotational relaxation time, and intrinsic viscosity studies of spectrin dimers (Mikkelsen et al., 1984) also support the description of spectrin as a flexible and extended molecule in solution.

Spectrin flexibility may have physiological significance since it may be related to the unique deformability and elasticity of erythrocytes. Several dynamic studies of spectrin, such as spin-labeling electron paramagnetic resonance (EPR) (Fung et al., 1979; Lemaigre-Dubreuil et al., 1980; Fung & Johnson, 1983; Dubreuil & Cassoly, 1983), nuclear magnetic resonance (NMR) (Calvert et al., 1980; Fung et al., 1986, 1989), time-resolved phosphorescence anisotropy (Learmonth et al., 1989), and transient dichroism (Clague et al., 1990), have shown that spectrin is motionally a highly flexible molecule that undergoes considerable local internal motions.

Dynamic light scattering (DLS) has been used extensively to investigate size, shape, and dynamics of biological macromolecules (Berne & Pecora, 1976; Lin & Schurr, 1978; Schurr & Schmitz, 1986; Bloomfield, 1985; Wilson et al., 1990). DLS experiments conducted in the near-ultraviolet (λ = 351.1 nm) have been employed to interrogate the dynamic behavior of macromolecules occurring on different time scales. Earlier DLS studies of spectrin provided information on translational diffusion coefficients and inferred from them a wormlike structure for spectrin molecules (Boe et al., 1979). In the present study, we employed DLS experiments to explore the dynamics of spectrin in dimer and tetramer equilibrium with the primary goal of acquiring evidence of internal or "segmental" motions within spectrin. DLS is able to detect a coexisting mixture of spectrin dimers and tetramers at several temperatures. Our results of DLS experiments conducted at a wavelength of 351.1 nm, over the temperature range from 23 to 41 °C, at scattering angles from 20° to 130° provide a means of simultaneously monitoring the solution dynamics of spectrin dimers and tetramers that occur on several different time and molecular length scales and provide further evidence for the presence of segmental motions in spectrin that occur over tens of microseconds (23 μs).

Materials and Methods

Preparation of Spectrin from Human Red Blood Cells. Human red blood cells (RBCs) were obtained from the local blood bank and used within 1 week of withdrawal. RBCs were washed three times with a 5 mM sodium phosphate buffer at pH 8.0 containing 150 mM NaCl. White membrane ghosts were prepared by lysing the washed RBCs with 20 volumes of a 5 mM sodium phosphate buffer at pH 8.0 and then washing the membrane three times with the same buffer, according to the published method (Dodge et al., 1963). The spectrin dimers, or tetramers, were prepared from the white membrane ghosts (Ungewickell & Gratzer, 1978). For dimer preparations, the membrane ghosts were washed once with a 0.3 mM sodium phosphate buffer at pH 7.6 (low ionic strength buffer), followed by incubation in the same buffer, at a concentration of about 2 mg/mL, for 30 min at 37 °C. For tetramer preparation, the membrane ghosts were dialyzed against the low ionic strength buffer overnight at 4 °C. The membrane samples were then centrifuged at 400000g in an ultracentrifuge for 20 min at 4 °C. The supernatant containing the spectrin–actin complex was pooled and concentrated with an ultrafiltration cell (Amicon) to a final concentration of about 1.5 mg/mL. This solution was loaded onto a Sepharose CL-4B column (Pharmacia) equilibrated with a 25 mM Tris buffer with 5 mM EDTA and 100 mM NaCl at pH 7.6. The spectrin dimers, or tetramers, were eluted at a flow rate of 22 mL/h for about 16 h. The dimer, or tetramer, fractions were pooled. To minimize nonessential handling of the protein samples, no further concentrating steps were used. Protein concentrations for the samples were determined, using an extinction coefficient value of 10 for a 1% spectrin solution at 280 nm (Marchesi et al., 1970; Clarke, 1971). Spectrin concentrations used were about 0.43 mg/mL for the dimer samples and 0.16 mg/mL for the tetramer samples. Unless specifically stated otherwise, all purification steps were carried out at 4 °C. SDS–polyacrylamide gel electrophoresis (Phast Gel, gradient 4–15, Pharmacia) was performed on the protein samples before and after DLS experiments. Overloaded gels verified that the spectrin samples were free of actin and other components, suggesting no change (degradation) of spectrin during the DLS measurements.

Preparations of Spectrin Samples for DLS Measurements. Spectrin solutions, either dimer or tetramer samples, were gently filtered through a 0.45-μm filter directly into a glass scattering cell that had been extensively rinsed with filtered buffer. The scattering cell was placed in the temperature-controlled cell holder (CIA Instruments, Bartlett, IL) of the apparatus and remained there for the duration of light scattering measurements. Each measurement took about 5 h. Temperature accuracy of the block heater is ±0.1 °C. For measurements at different temperatures, a fresh sample was used from the protein stock solution stored at 4 °C. The first measurement was collected at a scattering angle of 90° and again after 1.5 h into the experiment. If the measured diffusion coefficient values were the same (see below for details), the spectrin was presumed to have been temperature equilibrated at the start. If the later values changed by more than 1%, all previous measurements were repeated. At the greater times required for complete data collection slightly larger changes were observed, but there was never a change by more than 3% from the beginning to the end of any experiment.

DLS Measurements. Our experimental apparatus and data analysis methods have been recently described in detail (Wilson, et al., 1990; Benight et al., 1991). Briefly, the procedure employed for collection and analysis of DLS data is comprised of five steps. (1) Scattered photons are collected at angles, Θ, from 20° to 130° in the form of the intensity autocorrelation function $G^{(2)}(\mathbf{K},t)$, where $\mathbf{K}$ is the scattering vector and t is time. The angular dependence of $G^{(2)}$ enters through $\mathbf{K}$, since $\mathbf{K} = (4\pi n/\lambda_o) \sin(\Theta/2)$, where λ_o is the wavelength of the incident light in vacuo (351.1 nm) and n is the refractive index of the solvent, which has a value of 1.348. (2) After establishment of the $G^{(2)}(\mathbf{K},t)$ baseline, the curve is normalized with respect to this baseline and converted to the field correlation function, $g^{(1)}(\mathbf{K},t)$. Strategies for establishing an accurate and reliable baseline are described below. (3) $g^{(1)}$ is first fit with a single exponential function using the preexponential factor (amplitude) and relaxation rate as adjustable parameters in the fit. The goodness of the fit obtained with a single exponential provides a qualitative indication of whether more than one component is contributing to the decay of $g^{(1)}$. (4) To ascertain the presence of multiple components, the baseline-normalized $g^{(1)}$ is expressed as a sum of exponentials and subjected to Laplace inversion analysis

using the histogram method with program EXSAMP (Bertero et al., 1985; Russo et al., 1988). In addition, several correlation functions obtained at various scattering angles were analyzed using the Laplace inversion program CONTIN (Provencher, 1982) and gave essentially identical results. (5) Using the amplitudes and relaxation rates suggested by Laplace inversion as starting values, $g^{(1)}$ is fit by nonlinear least squares with the appropriate sum of exponential functions (double or triple exponential) using the relaxation rates, Γ_i, and relative amplitudes, A_i, as adjustable parameters in the fit, according to the following equation: $g^{(1)}(\mathbf{K},t) = \sum A_i \exp[-(\Gamma_i t)]$.

The diffusion coefficients, D_i, are then determined according to $D_i = \Gamma_i/\mathbf{K}^2$. For example, for a double exponential fit, two values of D_i, D_1 and D_2, will be obtained. The D_i values were then divided by the ratio of $(T/\eta)/(293.15/\eta_{water})$, where T was the temperature of the measurement, η_{water} equals 1.002 cP, and η was the sample viscosity, which depends on temperature and was taken from tabulated values of the viscosity of 100 mM NaCl (Stokes & Mills, 1965) to give D_{20}. The D_{20} values were plotted versus $\mathbf{K}^2$. Thus, molecular motions over different dimensions can be monitored at different $\mathbf{K}^2$ values.

Baseline Strategies. Generally, baseline corrections were $a\sqrt{N}$, where a was constant at each scattering angle but decreased with increasing angle. At all angles a was ≤ 5. $\sqrt{N}$ was the experimental uncertainty, and N was the average number of counts in the baseline region of $G^{(2)}$. Essentially this number of counts was subtracted from each channel of the experimentally collected $G^{(2)}(\mathbf{K},t)$. As will be described in the results, baseline corrections were used to eliminate a third, low-amplitude (<5%) slow component from the correlation function that could be detected when no baseline corrections were used.

Results

Temperature-Dependent DLS Measurements. DLS measurements were collected for solutions of spectrin, prepared as dimers at 4 °C, at temperatures of 23, 30, 37, 39, and 41 °C over a range in $\mathbf{K}^2$ from 0.7×10^{10} cm^{-2} to 20×10^{10} cm^{-2}. Earlier studies showed that, at low temperatures, either dimers or tetramers are kinetically trapped and little interconversion occurs over periods of up to several days (Ungewickell & Gratzer, 1978). However, at temperatures above 25 °C the dimer–tetramer equilibrium is achieved within hours to minutes and is not highly temperature dependent. We fully expected to observe the presence of a coexisting mixture of both dimers and tetramers in our samples at temperatures above 25 °C.

The acquired diffusion coefficients, D_{app}, obtained from single exponential analysis of the DLS data collected on solutions of spectrin over the temperature range from 23 to 41 °C but scaled to 20 °C in water are plotted versus $\mathbf{K}^2$ in Figure 1. With the exception of the data at 23 °C, a gradual increase of D_{app} is seen over the entire range of $\mathbf{K}^2$. Since the kinetics of dimer–tetramer interconversion are extremely slow below 25 °C (Ungewickell & Gratzer, 1978), we expected that the samples, prepared as dimers at 4 °C, consisted of anomalously high concentrations of kinetically trapped dimers at 23 °C that give unusually high diffusion coefficients. Aside from this exception, the increases in the curves of D_{app} versus $\mathbf{K}^2$, seen with increasing temperature from 30 to 41 °C, are consistent with the known increase of spectrin dimers over these temperatures. The curve for spectrin tetramers with data obtained at 23 °C on samples prepared as tetramers is also shown in Figure 1 and serves to define the lower limit of D_{app} versus $\mathbf{K}^2$ determined from single exponential analysis. Furthermore,

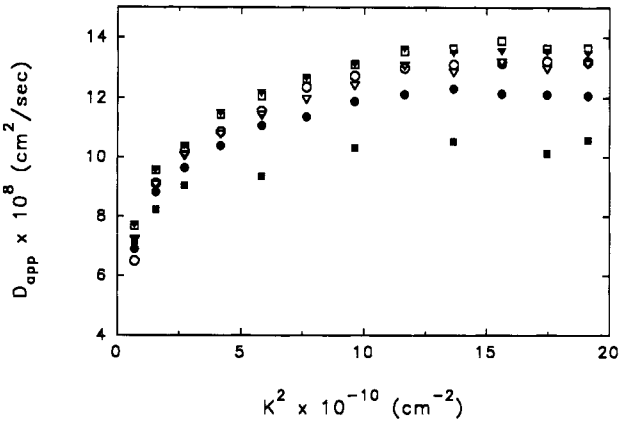

FIGURE 1: Plots of the diffusion coefficients D_{app} of spectrin prepared as dimers determined from force fitting a single exponential to the field autocorrelation functions collected as a function of $\mathbf{K}^2$ and temperature. Conditions for these experiments were 0.43 mg/mL spectrin in 100 mM NaCl, 25 mM Tris-HCl, and 5 mM EDTA, pH 7.4. Symbols for the curves for temperatures from 23 to 41 °C are as follows: 23 °C, open circles; 30 °C, closed circles; 37 °C, open triangles; 39 °C, closed triangles; 41 °C, open squares. The curve measured for a preparation of tetramers (0.16 mg/mL spectrin, identical buffer conditions) at 23 °C is also shown (closed squares) and defines the lower limits of the curves of D_{app} versus $\mathbf{K}^2$. Note, with the exception of the curve at 23 °C, for the dimer solutions a titratable increase of D_{app} versus $\mathbf{K}^2$ with temperature is observed.

since the temperature-dependent values of D_{app} in Figure 1 have all been scaled to 20 °C in water, the increases reveal actual changing dynamics of the spectrin species in solution. In order to assign these dynamical changes in terms of spectrin motions, the dimensions of spectrin dimers and tetramers in solution must be considered.

Spectrin dimers in solution have been proposed to adopt a wormlike coil configuration with a persistence length, P, of 17.4 nm at 30 °C (Elgsaeter et al., 1986; Stokke et al., 1985). The persistence length is a measure of the degree of flexibility of a polymer chain and is defined as the average extension along the z-axis of a chain that starts at the origin. Therefore, persistence lengths for polymers of identical contour lengths are at a maximum in the rigid rod and at a minimum in the random coil. The random coil is described as a chain containing N bonds of length b that are completely flexible. The orientation of one bond to the next is random. The wormlike coil falls between the two extremes defined by the random coil and rigid rod models. The root mean square (rms) radius of gyration, $\langle R_G^2\rangle^{1/2}$, of a wormlike coil can be determined from (Bloomfield et al., 1974)

$$\langle R_G^2\rangle^{1/2} = \{LP/3 - P^2 + 2P^3/L - 2P^4[1 - \exp(-L/P)]/L^2\}^{1/2} \quad (1)$$

where L is the contour length. The maximum extended contour lengths for dimers and tetramers (100 and 200 nm, respectively) were used to give an upper limit on R_G. Using a P value of 17.4 nm, eq 1 yields a maximum $\langle R_G^2\rangle^{1/2}$ of 19 nm for the dimer and 30 nm for the tetramer.

In DLS experiments of macromolecules, motions over different dimensions can be monitored at different $\mathbf{K}^2$ values. When the product $(\mathbf{K}R_G)^2 \leq 1$, D_{app} is largely a measure of the center of mass translational diffusion coefficient, D_0. If the global dimensions of the molecules are large enough such that the product $(\mathbf{K}R_G)^2 \gg 1$, D_{app} can conceivably arise from "segmental motions" within the molecules. Segmental motions are defined as motions faster than center of mass translational diffusion and include any subglobal motions that can appreciably contribute to the collected autocorrelation functions. Conceivably such motions can include overall rotations,

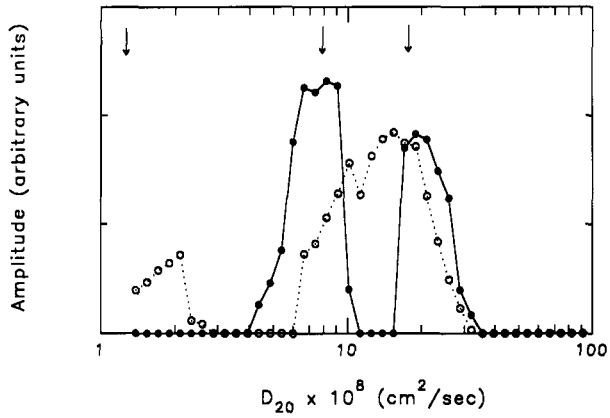

FIGURE 2: Results of Laplace inversion and exponential analysis of the field autocorrelation function collected on a solution of spectrin dimers at a scattering angle Θ of 40° and at 37 °C. The broken line is the distribution function of the temperature- and viscosity-corrected diffusion coefficients, D_{20} of spectrin obtained by Laplace inversion analysis of the collected field correlation function $g^{(1)}(\mathbf{K},t)$ without any baseline correction (see text). The solid line shows the distribution function obtained from Laplace inversion of $g^{(1)}(\mathbf{K},t)$ using a baseline correction of $a\sqrt{N}$ (a = 5; see text). The arrows at the top indicate the positions in the distribution of D_{20} values determined from fitting $g^{(1)}(\mathbf{K},t)$ with a three-exponential function. These results were typical of the DLS data collected on spectrin at scattering angles 40° through 130°.

bending, flexing, and twisting as well as translational motions of individual molecular segments along internal coordinates. Using the value of 19 nm for R_G(dimer), with $\mathbf{K}^2$ ranging from 0.7×10^{10} cm^{-2} to 20×10^{10} cm^{-2}, the product $(\mathbf{K}R_G)^2$ for dimers ranges from 0.03 to 0.72. Thus, D_0^{dim} will contribute to D_{app} over the entire range of $\mathbf{K}^2$. Segmental motions within dimers should only be significant in the experimentally inaccessible regions $\mathbf{K}^2 > 20 \times 10^{10}$ cm^{-2}. Alternatively, for tetramers, using the value of 30 nm for R_G(tetramer), $(\mathbf{K}R_G)^2$ ranges from 0.06 to 1.8. Thus, D_0^{tet} will be most influential when $(\mathbf{K}R_G)^2 \leq 1$, which corresponds to $\mathbf{K}^2 \leq 11 \times 10^{10}$ cm^{-2}. At $\mathbf{K}^2 > 11 \times 10^{10}$ cm^{-2}, segmental motions of tetramers should appreciably manifest in D_{app}. Within the confines of the wormlike coil model of spectrin, the plots of increasing D_{app} versus $\mathbf{K}^2$ in Figure 1 therefore potentially convey information regarding three classes of motions: translational motions of spectrin dimers and tetramers and segmental motions of tetramers. However, these three classes of motion cannot be directly resolved in Figure 1 since the results were obtained from a simple single exponential analysis of DLS data. Therefore, as described subsequently, Laplace inversion and multiexponential analysis of our collected DLS data are able to clearly resolve scattering contributions that are consistent with the three classes of motions.

Multiexponential Analysis of Spectrin. In order to obtain multiexponential analysis of DLS data collected on spectrin as a function of temperature, baseline adjustment and deconvolution were performed. Figure 2 shows typical plots of D_{20} and amplitude values obtained from Laplace inversion and exponential analysis of field correlation functions, $g^{(1)}$, collected at a scattering angle of 40° for solutions of spectrin at 37 °C. These data are representative of the DLS data collected over scattering angles from 40° to 130° at temperatures from 23 to 41 °C. Data collected at scattering angles of 20° and 30° will be described subsequently.

Two distribution functions of diffusion coefficients at 20 °C (D_{20}) as a function of their respective amplitudes are displayed in Figure 2. The broken line shows the D_{20} distribution of spectrin obtained directly from Laplace inversion of the $g^{(1)}(\mathbf{K},t)$ without any baseline correction. Three peaks are evident. These data indicate the presence of two predominant dynamic components (the faster peaks) and a minor component (the slowest peak) in the protein solution. The slowest peak ($D_{20} \leq 2.0 \times 10^{-8}$ cm^2/s) is well resolved from the other two with a considerably lower amplitude. The low amplitude and slow diffusion coefficient of the slowest peak suggest that it is probably due to a very small population of large protein oligomers or aggregates. The faster peaks at $D_{20} \approx 10 \times 10^{-8}$ cm^2/s and 16×10^{-8} cm^2/s are overlapping. The solid line shows the distribution function obtained from Laplace inversion of the DLS data with a baseline correction of $a\sqrt{N}$ (a = 5). To determine the optimum value of a at each scattering angle, baseline corrections were progressively increased until the slow peak vanished from the distribution. Data collected at different scattering angles required different baseline corrections to eliminate the slowest component, but corrections were never greater than a = 5. After baseline correction, the slow peak is absent from the distribution function and the peaks of the faster components are more resolved. D_{20} of the slower component decreases to $\approx 7.3 \times 10^{-8}$ cm^2/s. D_{20} of the faster peak increases to $\approx 20.3 \times 10^{-8}$ cm^2/s. This shifting of the peaks upon Laplace inversion of the baseline-corrected $g^{(1)}(\mathbf{K},t)$'s was observed to varying extents at every temperature and nearly all values of $\mathbf{K}^2$. Such artifacts are unfortunately inherent in multiexponential analysis of DLS data and therefore introduce an experimental uncertainty in the evaluated D_{20}'s of the faster components. In this regard, the reported D_{20} values of these faster components should, in general, be considered to be no more accurate than $\pm 2 \times 10^{-8}$ cm^2/s.

As an independent check of the diffusion coefficients obtained by Laplace inversion using a baseline correction, all data were also fit with triexponential functions without baseline correction. The arrows in Figure 2 indicate the position in the distribution of the D_{20}'s obtained by this procedure at Θ = 40°. The normalized amplitudes of the exponential components are 0.05, 0.60, and 0.35 for the slowest and two faster peaks, respectively, indicating the fractional contribution of each component to $g^{(1)}$ at this angle. The excellent agreement observed between the D_{20}'s obtained from the triexponential fit and the baseline-corrected Laplace inversion validates the method of baseline correction. The same data were also fit with a biexponential function without baseline correction. An F-test supported the triexponential over the biexponential fit at a 95% confidence level. In addition, data obtained at all other temperatures and scattering angles analyzed in a similar manner supported the triexponential fits at confidence levels ≥95%.

Data collected at scattering angles of 20° and 30° were subjected to Laplace inversion without baseline corrections because at these angles large corrections ($\gg 5\sqrt{N}$) would have been required. At Θ = 30°, distribution functions were similar to that shown in Figure 2 obtained at Θ = 40° (and larger angles) without baseline correction; i.e., a small slow peak ($D_{20} = 2.5 \times 10^{-8}$ cm^2/s) and a broad main peak ($D_{20} = 13.7 \times 10^{-8}$ cm^2/s) were observed. At Θ = 20° (no baseline correction), the broad peak was resolved into two main peaks resulting in three peaks on the distribution. The slowest peak had a relatively small amplitude just as observed at higher angles. The two main peaks had approximately equal amplitudes with D_{20}'s = 19.8×10^{-8} cm^2/s and 7.5×10^{-8} cm^2/s. The agreement between the diffusion coefficients obtained by Laplace inversion at Θ = 20° without baseline correction, those obtained at angles of 40° (and 50°) with baseline correction, and those obtained by exponential fitting at these angles

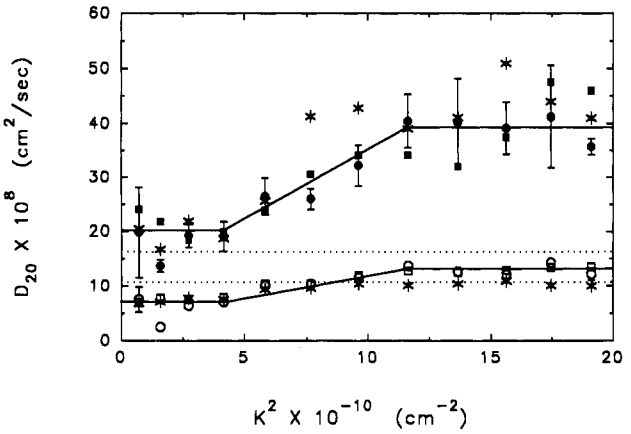

FIGURE 3: Diffusion coefficients of the fast (closed symbols) and slow (open symbols) components obtained by Laplace inversion (circles) and a three-exponential analysis (squares) of the collected $g^{(1)}(\mathbf{K},t)$'s at scattering angles from 20° to 130° in 10° increments. Values were viscosity and temperature corrected, averaged over five temperatures at each angle, and then plotted versus $\mathbf{K}^2$. Exponential data are from a three-exponential fit; the slowest exponential ($D_{20} \leq 2 \times 10^{-8}$ cm^2/s) is not shown. Three distinct regions of the curves are evident. As described in the text, if spectrin is modeled as a wormlike coil, translational diffusion of the center of mass of spectrin dimers and tetramers is assigned to the slow component over the whole range of $\mathbf{K}^2$. In the high $\mathbf{K}^2$ region, the fast component is attributed to segmental motions of spectrin. The reproducibility of the data is demonstrated by the curve of $D_{20}(\mathbf{K}^2)$ versus $\mathbf{K}^2$ (asterisks) collected on a spectrin sample from a different preparation (0.62 mg/mL, identical buffer conditions). The dotted lines indicate the dimer (upper line) and tetramer (lower line) translational diffusion coefficients, D_0, determined from published s values of spectrin dimers and tetramers using the Svedberg equation as described in the text.

provided further evidence for the validity of our baseline correction scheme.

Within the uncertainty stated above, the temperature dependence of the D_{20} values of spectrin was relatively small. Diffusion coefficients averaged over all temperatures at each value of $\mathbf{K}^2$, $D_{20}(\mathbf{K}^2)$, for the faster components in the distribution functions of Figure 2 are plotted versus $\mathbf{K}^2$ in Figure 3. The error bars indicate the deviations from the average D_{20}'s over the temperature range from 23 to 41 °C. The slowest component determined from exponential fitting ($D_{20} < 2 \times 10^{-8}$ cm^2/s) is not shown. Reproducibility of the results is demonstrated by the similar $D_{20}(\mathbf{K}^2)$ values determined from DLS measurements of two separate preparations of spectrin samples.

The curves in Figure 3 reveal several interesting characteristics of the behavior of spectrin in these DLS experiments. (1) Comparable D_{20} values for the fast and slow components are obtained over the entire range of $\mathbf{K}^2$ by both Laplace inversion analysis and exponential fitting. (2) For both the fast and slow components, three distinct regions of the curve of D_{20} versus $\mathbf{K}^2$ are evident. In the low $\mathbf{K}^2$ region (0.7×10^{10} cm$^{-2} \leq \mathbf{K}^2 \leq 4 \times 10^{10}$ cm^{-2}) the diffusion coefficient of the slow component is constant, with values of $(7.3 \pm 2.0) \times 10^{-8}$ cm^2/s. Over this same region, the fast-component diffusion coefficient is also constant, with values of $(20.3 \pm 2.0) \times 10^{-8}$ cm^2/s. In the high $\mathbf{K}^2$ region (11×10^{10} cm$^{-2} \leq \mathbf{K}^2 \leq 20 \sim 10^{10}$ cm^{-2}), D_{20} of the slow component is $(13.0 \pm 2.0) \times 10^{-8}$ cm^2/s, and D_{20} of the fast component is $(39.4 \pm 2.0) \times 10^{-8}$ cm^2/s. In the intermediate zone of the curves (4×10^{10} cm$^{-2} < \mathbf{K}^2 < 11 \times 10^{10}$ cm^{-2}) D_{20} is a linear function of $\mathbf{K}^2$ and appears as a transition region between the low and high $\mathbf{K}^2$ regions.

Segmental Motions in Spectrin. Since it was our primary goal to investigate the potential existence of subglobal segmental motions in spectrin, it was essential to determine which components and respective regions of the curves in Figure 3 could be attributed to global translational motions of the spectrin dimers and tetramers. If the molecular weight and sedimentation coefficient (s) of a macromolecule are known, the translational diffusion coefficient can be calculated using the Svedberg equation:

$$D_0 = sN_0kT/M(1 - \bar{v}\rho_0)$$

where N_0 is Avogadro's number, k is Boltzmann's constant, T is the absolute temperature, M is the molecular weight, $\bar{v}$ is the partial specific volume, and ρ_0 is the density of the solution. For spectrin, $\bar{v}$ is 0.733 mL/g (Kam et al., 1977), s of spectrin dimers is 9.5 ± 0.5 S and of spectrin tetramers is 12.5 ± 0.5 S (Kam et al., 1977), and M is 531 000 for spectrin dimers (Sahr et al., 1990; Winkelmann et al., 1990). The Svedberg equation yields D_0^{dim} of $(16.3 \pm 0.8) \times 10^{-8}$ cm^2/s and D_0^{tet} of $(10.7 \pm 0.4) \times 10^{-8}$ cm^2/s. In light of these calculations and considering the arguments stated above concerning the overall dimensions of spectrin dimers and tetramers in wormlike coil configurations, the behavior of the fast and slow components in the three regions of the curves in Figure 3 can be assigned to three classes of motions of the spectrin molecules.

As previously stated, in the low $\mathbf{K}^2$ region ($0 \leq \mathbf{K}^2 \leq 4 \times 10^{10}$ cm^{-2}) segmental motion should not contribute to the observed signal, and translational diffusion of both spectrin dimers and tetramers should be observed. Considering the experimental uncertainties and assumptions involved, the constant value of the fast component [$(20.3 \pm 2.0) \times 10^{-8}$ cm^2/s] in this region is only slightly higher than D_0^{dim} calculated above. Therefore, the fast component in the low $\mathbf{K}^2$ region is taken to be due to center of mass diffusion of the spectrin dimer. In the same token, the constant value of the slow component in the low $\mathbf{K}^2$ region [$(7.3 \pm 2.0) \times 10^{-8}$ cm^2/s] is slower than D_0^{tet} calculated above from sedimentation data. This could be due to a small amount of higher order spectrin oligomers whose contribution to the scattered signal was not removed by baseline correction. Therefore, the slow component in the low $\mathbf{K}^2$ region is attributed mainly to the center of mass diffusion of the spectrin tetramer, D_0^{tet}. In the high $\mathbf{K}^2$ region (11×10^{10} cm$^{-2} \leq \mathbf{K}^2 \leq 20 \times 10^{10}$ cm^{-2}) the slow component (13.0×10^{-8} cm^2/s) is attributed to an average of D_0^{tet} and D_0^{dim}. The extraordinary increase of the fast component (39.4×10^{-8} cm^2/s) indicates the emergence of much faster, probably segmental motions of the tetramer detected when $(\mathbf{K}R_G)^2 > 1$. On the basis of the average value of $D_{20} \approx 39.4 \times 10^{-8}$ cm^2/s of the fast component in this region, these motions have a relaxation time, $\tau \leq 1/D_{20}\mathbf{K}^2 = 23$ μs. Since the displayed values are temperature averaged, the large error bars of the fast component in the high $\mathbf{K}^2$ region indicate a significant temperature dependence of these motions and probably reveal that more than one type of segmental motion is being monitored in this region. Assignment of the intermediate region of the curves in Figure 3 (4×10^{10} cm$^{-2} < \mathbf{K}^2 < 11 \times 10^{10}$ cm^{-2}) is more ambiguous. Considering the assignments of the adjoining low and high $\mathbf{K}^2$ regions, the slow component must be an unresolvable combination of D_0^{dim} and D_0^{tet}, while the fast component is probably due to a mixture of all three types of spectrin motion that cannot be resolved. The normalized amplitudes of the fast and slow components support these assignments.

Figure 4 shows the normalized amplitudes of the fast and slow components of Figure 3 as a function of $\mathbf{K}^2$. Normalized amplitudes from DLS experiments are a measure of the fractional contribution of a particular motion to $g^{(1)}$ and do

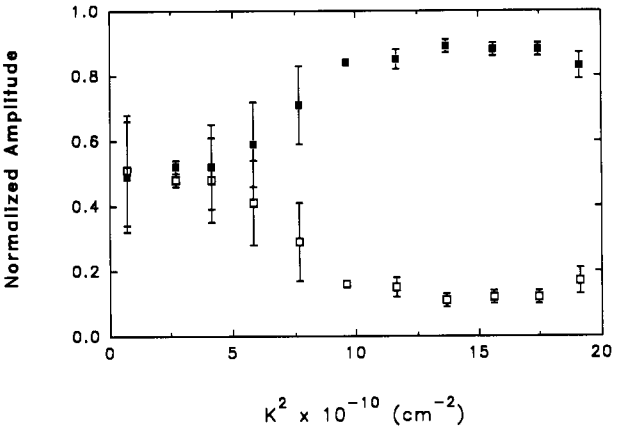

FIGURE 4: Average normalized amplitudes of the fast (open squares) and slow (closed squares) components of Figure 3 as a function of $\mathbf{K}^2$. The behavior of these amplitudes is consistent with the assignments given in Figure 3 (see text).

not in themselves indicate the exact population of a particular species present in solution. The behavior of these amplitudes in the present experiments is consistent with the assignments of the slow and fast components to dynamic motions of spectrin given above. In the low $\mathbf{K}^2$ region the fast and slow components (20.3×10^{-8} cm^2/s and 7.3×10^{-8} cm^2/s) have equal amplitudes ($\approx$0.50), revealing a mixture of spectrin dimers and tetramers. In the intermediate region, the fast-component amplitude decreases to 0.20 while the slow-component amplitude concomitantly increases to 0.80. These changes are consistent with a mixture of center of mass motions of dimers and tetramers and internal motions of tetramers. As $\mathbf{K}^2$ increases, the average center of mass diffusion of the dimers and tetramers becomes the dominant slow component. The fast component corresponding to segmental motions of the spectrin tetramers is overshadowed by the slow component, and its amplitude decreases, paralleling the increases of the slow-component amplitude. In the high $\mathbf{K}^2$ region the amplitudes of the slow component (13.0×10^{-8} cm^2/s, average center of mass translation) and fast component (39.3×10^{-8} cm^2/s, internal motions of tetramers) are constant.

Comparisons with Other DLS Studies of Spectrin. DLS experiments of spectrin conducted under conditions similar to those employed in our study have been reported by Boe et al. (1979). These studies were conducted at 514.5 nm over an angular range from 30° to 130° (2.2×10^{10} cm$^{-2} < \mathbf{K}^2 < 8.7 \times 10^{10}$ cm^{-2}). Data were obtained on samples prepared separately as dimers and as tetramers. The authors did not perform Laplace inversion or multiexponential analysis of these data; rather a single relaxation rate (Γ) was obtained at each angle by fitting a semilog plot of the correlation function. Afterward, plots of Γ versus $\mathbf{K}^2$ were made. D_{20} values for spectrin dimers and tetramers were taken as the slopes of these lines, and data were taken as a function of temperature and protein concentration. The translational diffusion coefficients of dimers and tetramers were then taken as the intercepts of plots of D_{20} versus protein concentration. By this analysis, these authors found $D_0^{tet} = (9.5 \times 0.8) \times 10^{-8}$ cm^2/s, which is equal to our value within experimental error. Their value of D_0^{dim} is $(14.0 \pm 0.5) \times 10^{-8}$ cm^2/s, which is lower than our value. This difference could be due to small populations of tetramers or higher oligomers present in their samples.

To further compare these two studies, we subjected our DLS data to a similar analysis by fitting the electric field autocorrelation functions $g^{(1)}(\mathbf{K},t)$ to a single exponential decay, plotting the resulting decay rates versus $\mathbf{K}^2$, and taking D_{20} as the slope of these lines. This analysis was performed on the data obtained at 23 °C for the protein solution prepared as dimers and the protein solution prepared as tetramers. This analysis gave $D_0^{dim} = (13.7 \pm 0.1) \times 10^{-8}$ cm^2/s and $D_0^{tet} = (10.3 \pm 0.1) \times 10^{-8}$ cm^2/s. The results of Boe et al. (1979) were $D_0^{dim} = (13.8 \pm 0.2) \times 10^{-8}$ cm^2/s and $D_0^{tet} = (10.0 \pm 0.2) \times 10^{-8}$ cm^2/s (interpolated to match our protein concentrations). Such agreement indicates that nearly identical protein solutions were used by us and these authors. In addition, our DLS experiments conducted in the ultraviolet and subjected to Laplace/exponential analysis revealed the presence of segmental motions of spectrin.

When these results are compared, the uncertainties obtained should be noted. The uncertainties given by Boe and coworkers above are lower than our value of $\pm 2.0 \times 10^{-8}$ cm^2/s. The difference between these numbers does not indicate that our experiments were less accurate than theirs. The accuracy of our apparatus is actually better in comparison, mainly due to the capacity of our correlator (272 versus 24 channels). This increase in channel number yields a much lower noise level. The difference in the reported uncertainties arises due to different ways in determining uncertainties. Boe and coworkers calculated their uncertainty from the reproducibility between experiments. As indicated in Figure 3, our results also exhibit excellent reproducibility. However, our uncertainty ($\pm 2.0 \times 10^{-8}$) is estimated from the error involved in fitting the function by Laplace inversion. In the low $\mathbf{K}^2$ region the error is high because the peaks being separated differ only by a factor of 3. Under the most optimum conditions, this data analysis can at best separate peaks differing by a factor of 2. Therefore, we are near the limit of its applicability. In the high $\mathbf{K}^2$ region the fast peak has a low amplitude and a high decay rate, also pushing the limit of the analysis routine. These combined effects were estimated to give rise to our reported uncertainties. Force fitting to a single exponential yields small uncertainties ($\pm 0.1 \times 10^{-8}$) for our data also because the diffusion coefficients determined in this way are "averaged" over all solution components. If two solutions have the same distribution, they will yield the same diffusion coefficient because there is little error inherent in force fitting one exponential. However, this form of data analysis cannot yield the true distribution and therefore is not as accurate in determining diffusion coefficients when more than one species is present in solution.

Discussion

Protein molecules consist of a large number of groups linked by covalent bonds that possess a large number of rotational degrees of freedom. The groups, such as CONH peptide groups or the ring in the tyrosine side chain, linked by such bonds are themselves comparatively rigid and constitute the fundamental dynamical elements in a protein molecule. The typical thermal motions observed within a protein are dominated by the torsional oscillations of these groups about the single bonds that link them together. Superposition of the rigid group displacements yields a remarkably rich dynamic spectrum that ranges from the rapid local motions of individual groups to slow collective distortions of large regions within the molecule. Specific motions, with characteristic times ranging from 10^{-14} s to seconds, have been studied in many proteins to provide significant insight toward understanding the functional properties of these proteins (McCammon & Harvey, 1987). The ultrastructure of spectrin reveals that spectrin is a flexible molecule. The flexibility of spectrin is significant for its function. It has been suggested that spectrin flexibility plays an important role in determining the deformability and elasticity of the erythrocyte (Vertessy & Steck, 1989). It has

also been suggested that, as a consequence of the flexibility of spectrin, the linkage of band 3 to the skeleton does not act as a restraint on band 3 rotational motion (Clague et al., 1989). However, the study of spectrin dynamics is still in its infancy, as compared to many other proteins, such as myosin (Barnett & Thomas, 1989; Sommerville et al., 1990). Our present studies of spectrin dynamics, with an improved treatment of the DLS data obtained, reveal the translational diffusion coefficients of spectrin in solution, with dimers and tetramers in equilibrium, and provide evidence of internal or segmental motions within spectrin.

Early spin-label EPR studies showed that saturation-transfer detection, with a time scale of 10^{-6} to 10^{-3} s, was sensitive to the dynamics of spectrin and that the molecular motions appear to be unrestricted by other membrane components (Fung et al., 1979). Subsequent studies showed that spin-labeled spectrin dimers and tetramers had similar rotational dynamics in solution, in the microsecond range at 2 °C (Lemaigre-Dubreuil et al., 1980; Dubreuil et al., 1983). The results also confirmed that the dynamics of spectrin remain the same in samples associated to membrane-bound ankyrin.

The main difference between this work and the previous DLS study of spectrin (Boe et al., 1979) is our treatment of the solution as a distribution of diffusing species rather than having one "average" decay rate. The Laplace inversion analysis allows us to see the distribution of decay rates contributing to the signal. This data analysis technique yields reliable information only when the data have low noise levels. We were able to achieve these low noise levels by using solutions that are as homogeneous as possible and by utilizing a correlator with a large number (272) of channels. In addition, the use of ultraviolet light (351.1 nm) allows access to the high $\mathbf{K}^2$ range where internal motions could be detected. The previous study (Boe et al., 1979) was conducted at $\mathbf{K}^2 \leq 10 \times 10^{10}$ cm^{-2} with a 24-channel correlator. Thus we believe that our analysis represents an improved DLS investigation of spectrin. Consequently, the previously reported translational diffusion coefficients were higher than our value of $(7.3 \pm 2.0) \times 10^{-8}$ cm^2/s for the tetramers, probably because there were some dimers in the solution. Similarly, the diffusion coefficients of the dimers were lower than our value of $(20.3 \pm 2.0) \times 10^{-8}$ cm^2/s, probably because the diffusion coefficients for tetramers in solution were averaged in.

Our DLS experiments suggest the presence of segmental spectrin motions. Studies with EPR indicated that spectrin exhibited multiple classes or rates of motion (Fung & Johnson, 1983). The three principal motional components appear to have correlation times of $\leq 10^{-9}$ s, 10^{-7} to 10^{-6} s, and about 10^{-3} s. The proportion of fast component ($\leq 10^{-9}$ s) is quite sensitive to pH over the pH range from 6 to 8 and moderately sensitive to temperature over the range 0–34 °C. At pH 8 and 20 °C it comprises about 10% of the total spectral intensity. The relative proportions of slow and very slow components appear moderately sensitive to temperature but virtually independent of pH over the range 6–8. NMR studies demonstrate rapid segmental motions (10^{-10} to 10^{-9} s) as well as relatively slow motions (slower than microseconds) in spectrin (Fung et al., 1986, 1989). Phosphorescence anisotropy studies reveal for spectrin dimers a rotational correlation time of 3 μs and relaxation times of 3 and 30 μs for spectrin tetramers at 10 °C (Learmonth et al., 1989), whereas transient dichroism studies of spectrin gave a correlation time of about 10^{-4} s, at 4 °C (Clague et al., 1990). All measurements to date agree that spectrin molecules exhibit internal motions and that the internal motions of spectrin are largely preserved upon binding to the erythrocyte membrane. The segmental motions detected in the present DLS study, with D_{20} of $(39.4 \pm 2.0) \times 10^{-8}$ cm^2/s, or $\tau \sim 23$ μs, are attributed to these subglobal thermal fluctuations of segments within spectrin tetramers. This motion was assigned on the assumption of a wormlike coil model for spectrin, with persistence length of 17.4 nm, contour length of 100 nm, and radius of gyration of 19 nm for the dimer. Thus DLS data suggest that spectrin molecules fluctuate over the distance of $1/\mathbf{K}$, about 30 nm for $\mathbf{K}^2$ of 11×10^{10} cm^{-2}, or 22 nm for $\mathbf{K}^2$ of 20×10^{10} cm^{-2}, with relaxation times around 23 μs or shorter. These motions are relatively large and amount to about one-fifth of the total contour length of the dimer. These DLS results are in good agreement with recent electron microscopic studies of spectrin which suggested the protein is extremely flexible with thermally induced fluctuations able to increase the helix contour length by as much as 60% (McGough & Josephs, 1990). The motions are likely to be complex and could include rotations, torsions, and bending motions, as well as translations along internal coordinates. All experimental data to date indicate that these local thermal fluctuations of spectrin subunits, internal or segmental motions, relax to their mean equilibrium position on time scales between 100 ps and 100 μs.

In this paper, it was not our intention to provide quantitative assignments of such motions in terms of local structural fluctuations of spectrin. Interpretation of the data is consistent with a wormlike coil model of spectrin. Since most proteins can exist in several conformations and aggregation states, and DLS has the ability within limitations to observe multiple diffusion states simultaneously, DLS should emerge as a potentially powerful and novel technique for studying the structure and dynamics of normal and mutant spectrin molecules. For example, DLS techniques can be applied to study spectrin flexibility under experimental conditions that have been observed to give extended or contracted configurations, which may play an important role in the deformability of erythrocyte (Vertessy & Steck, 1989).

References

Barnett, V. A., & Thomas, D. D. (1989) *Biophys. J. 56*, 517–523.

Benight, A. S., Wilson, D. H., Budzynski, D. M., & Goldstein, R. F. (1991) *Biochimie 73*, 143–155.

Bennett, V., & Lamber, S. (1991) *J. Clin. Invest. 87*, 1483–1489.

Berne, B. J., & Pecora, R. (1976) *Dynamic Light Scattering*, John Wiley & Sons, New York.

Bertero, M., Brianzi, P., Pike, E. R., de Villers, G., Lan, K. H., & Ostrowsky, N. (1985) *J. Chem. Phys. 82*, 1551–1554.

Bloomfield, V. A. (1985) in *Dynamic Light Scattering, Applications of Photon Correlation Spectroscopy* (Pecora, R., Ed.) pp 363–416, Plenum Press, New York.

Bloomfield, V. A., Crothers, D. M., & Tinoco, I., Jr. (1974) *Physical Chemistry of Nucleic Acids*, p 161, Harper and Row, New York.

Boe, A., Elgsaeter, A. A., Oftedal, G., & Strand, K. (1979) *Acta Chem. Scand., Ser. A 33*, 245–249.

Byers, T. J., & Branton, D. (1985) *Proc. Natl. Acad. Sci. U.S.A. 82*, 6153–6157.

Calvert, R., Bennett, P., & Gratzer, W. (1980) *Eur. J. Biochem. 107*, 363–367.

Clague, M. J., Harrison, J. P., Morrison, I. E. G., Wyatt, K. J., & Cherry, A. J. (1990) *Biochemistry 29*, 3898–3904.

Clarke, M. (1971) *Biochem. Biophys. Res. Commun. 45*, 1063–1070.

Davison, M. D., & Critchley, D. R. (1989) *Cell 52*, 150–159.

Davison, M. D., Baron, M. D., Critchley, D. R., & Wootton, J. C. (1989) *Int. J. Biol. Macromol. 11*, 81–90.
Dodge, J. T., Mitchell, D., & Hanahan, D. J. (1963) *Arch. Biochem. Biophys. 100*, 119–130.
Dubreuil, Y. L., & Cassoly, R. (1983) *Arch. Biochem. Biophys. 223*, 495–502.
Elgsaeter, A. (1978) *Biochim. Biophys. Acta 536*, 235–244.
Elgsaeter, A., Stokke, B. T., Mikkelsen, A., & Branton, D. (1986) *Science 234*, 1217–1223.
Fung, L. W.-M., & Johnson, M. E. (1983) *J. Magn. Reson. 51*, 233–244.
Fung, L. W.-M., SooHoo, M. J., & Meena, W. A. (1979) *FEBS Lett. 105*, 379–383.
Fung, L. W.-M., Lu, H.-Z., Hjelm, R. P., Jr., & Johnson, M. E. (1986) *FEBS Lett. 197*, 234–238.
Fung, L. W.-M., Lu, H.-Z., Hjelm, R. P., Jr., & Johnson, M. E. (1989) *Life Sci. 44*, 735–740.
Kam, Z., Josephs, R., Eisenberg, H., & Gratzer, W. B. (1977) *Biochemistry 16*, 5568–5572.
Koenig, M., Monaco, A. P., & Kunkel, L. M. (1988) *Cell 53*, 219–228.
Learmonth, R. P., Woodhouse, A. G., & Sawyer, W. H. (1989) *Biochim. Biophys. Acta 987*, 124–128.
Lemaigre-Dubreuil, Y., Henry, Y., & Cassoly, R. (1980) *FEBS Lett. 113*, 231–234.
Lin, S.-C., & Schurr, J. M. (1978) *Biopolymers 17*, 425–461.
Marchesi, S. L., Steers, E., Marchesi, V. T., & Tillach, W. T. (1970) *Biochemistry 9*, 50–57.
Marchesi, V. T. (1985) *Annu. Rev. Cell Biol. 1*, 531–561.
McCammon, J. A., & Harvey, S. C. (1987) *Dynamics of Proteins and Nucleic Acids*, Cambridge University Press, Cambridge.
McGough, A. M., & Josephs, R. (1990) *Proc. Natl. Acad. Sci. U.S.A. 87*, 5208–5212.
Mikkelsen, A., & Elgsaeter, A. (1978) *Biochim. Biophys. Acta 536*, 245–251.
Mikkelsen, A., & Elgsaeter, A. (1981) *Biochim. Biophys. Acta 668*, 74–80.
Mikkelsen, A., Stokke, B. T., & Elgsaeter, A. (1984) *Biochim. Biophys. Acta 786*, 95–102.
Morris, M., & Ralston, G. B. (1989) *Biochemistry 28*, 8561–8567.
Provencher, S. W. (1982) *Comput. Phys. Commun. 27*, 213–229.
Ralston, G. B. (1976) *Biochim. Biophys. Acta 455*, 163–172.
Ralston, G. B. (1978) *J. Supramol. Struct. 8*, 361–373.
Ralston, G. B. (1991) *Biochemistry 30*, 4179–4186.
Russo, P., Guo, K., & Delong, L. (1988) *Conference Proceedings of the Society of Plastics Engineers, ANTIEC*, pp 983–985, Society of Plastics Engineers, Brookfield, CT.
Sahr, K. E., Laurila, P., Kotula, L., Scarpa, A. L., Coupal, E., Leto, T. L., Linnenbach, A. J., Winkelmann, J. C., Speicher, D. S., Marchesi, V. T., Curtis, P. J., & Forget, B. G. (1990) *J. Biol. Chem. 265*, 4434–4443.
Schurr, J. M., & Schmitz, K. S. (1986) *Annu. Rev. Phys. Chem. 37*, 271–305.
Shahbakhti, R., & Gratzer, W. B. (1986) *Biochemistry 25*, 5969–5975.
Shotton, D. M., Burke, B. E., & Brank, D. J. (1979) *J. Mol. Biol. 131*, 303–329.
Sommerville, L. E., Henry, G. D., Sykes, B. D., & Hartshorne, D. J. (1990) *Biochemistry 29*, 10855–10864.
Speicher, D. V., & Marchesi, V. T. (1984) *Nature 311*, 177–180.
Speicher, D. V., Gary, D., & Marchesi, V. T. (1983) *J. Biol. Chem. 258*, 15938–15947.
Stokes, R. H., & Mills, R. (1965) in *The International Encyclopedia of Physical Chemistry and Chemical Physics* (Stokes, R. H., Ed.) Topic 16, Vol. 3, p 118, Pergamon Press, New York.
Stokke, B. T., Mikkelsen, A., & Elgsaeter, A. (1985) *Biochim. Biophys. Acta 816*, 102–110.
Stokke, B. T., Mikkelsen, A., & Elgsaeter, A. (1986) *Biophys. J 49*, 319–327.
Ungewickell, E., & Gratzer, W. (1978) *Eur. J. Biochem. 88*, 379–385.
Vertessy, B. G., & Steck, T. L. (1989) *Biophys. J. 55*, 255–262.
Wasenius, W., Saraste, M., Salven, P., Eramaa, M., Holm, L., & Lehto, V. (1989) *J. Cell Biol. 108*, 79–93.
Waugh, R. E. (1982) *Biophys. J. 39*, 273–278.
Wilson, D. H., Price, H. L., Henderson, J., Hanlon, S., & Benight, A. S. (1990) *Biopolymers 29*, 357–376.
Winkelmann, J. C., Chang, J.-G., Tse, W. T., Scarpa, A. L., Marchesi, V. T., & Forget, B. G. (1990) *J. Biol. Chem. 265*, 11827–11832.
Xu, Y., Prabhakaran, M., Johnson, M. E., & Fung, L. W.-M. (1990) *J. Biomol. Struct. Dyn. 8*, 55–62.